Proc. Indian Acad. Sci. (*Chem. Sci.*), Vol. 115, Nos 5 & 6, October–December 2003, pp 341–348

Electrical conduction in composites containing copper core–copper oxide shell nanostructure in silica gel[¶]

D DAS[a], T K KUNDU[b], M K DEY[c], S CHAKRABORTY[a] and D CHAKRAVORTY[a,*]

[a]Indian Association for the Cultivation of Science, Jadavpur, Kolkata 700 032, India

[b]Department of Physics and Technophysics, Vidyasagar University, Midnapore 721 102, India

[c]Variable Energy Cyclotron Centre, Sector I, AF Bidhan Nagar, Kolkata 700 064, India

e-mail: mlsdc@mahendra.iacs.res.in

Abstract. Composites of nanometre-sized copper core–copper oxide shell with diameters in the range 6·1 to 7·3 nm dispersed in a silica gel were synthesised by a technique comprising reduction followed by oxidation of a suitably chosen precursor gel. The hot pressed gel powders mixed with nanometre-sized copper particles dispersed in silica gel showed electrical resistivities several orders of magnitude lower than that of the precursor gel. Electrical resistivities of the different specimens were measured over the temperature range 30 to 300°C. Activation energies for the core-shell nanostructured composites were found to be a fraction of that of the precursor gel. Such dramatic changes are ascribed to the presence of an interfacial amorphous phase. The resistivity variation as a function of temperature was analysed on the basis of Mott's small polaron hopping conduction model. The effective dielectric constant of the interfacial phase as extracted from the data analysis was found to be much higher than that of the precursor glass. This has been explained as arising from the generation of very high pressure at the interface due to the oxidation step to which the copper nanoparticles are subjected.

Keywords. Copper core–copper oxide shell; electrical conduction in composites; nanostructures.

1. Introduction

Nanostructured materials have been studied extensively in recent years because of new physics expected from them and exotic properties exhibited by these systems.[1–4] Nanocrystalline materials have the characteristic feature of a large surface-to-volume ratio and hence contain a high volume fraction of grain boundaries. The films in these regions have been used to study the structure and dynamics of films in confined geometries.[5] Molecular dynamics simulation investigations of silicon grain boundaries indicate the existence of an amorphous equilibrium structure.[6,7] We have grown a metal core–metal oxide shell structure with nanoscale dimensions within a silica gel. The percolative configuration of the composite nanoparticles generates a large interface in the disordered

[¶]Dedicated to Professor C N R Rao on his 70th birthday

*For correspondence

medium. The drastic change in electrical conductivity of the resultant structure as compared to that of the parent gel indicates the marked influence of the interfaces on the transport properties of this system. We describe the details in this paper.

2. Experimental

The metallic species used in the present investigation was copper. The target gel composition was chosen such that after reducing it the copper phase formed a percolative structure. Accordingly the target composition for preparing the composites in this study was $60CuO{\cdot}40SiO_2$ (in mole%). $CuCl_2{\cdot}2H_2O$ and $Si(OC_2H_5)_4$ were used as precursors. 60 ml of ethyl alcohol was mixed with 10 ml distilled water and 1 ml HCl. The solution was stirred for 10 min and then 12·5 ml of $Si(OC_2H_5)_4$ was added. The stirring was continued for 1 h. Another solution was prepared by mixing 14·26 g of $CuCl_2{\cdot}2H_2O$ with 60 ml C_2H_5OH and 15 ml distilled water and stirred for 20 min. The two solutions prepared as above were mixed and stirred for 1 h. The mixture was left as such for a few days for gelation. The resultant gel was reduced in hydrogen at 650°C for 30 min. This gave rise to precipitation of metallic copper of nanometer dimensions within the gel matrix.[8] The powders resulting from this step were hot pressed at 650°C for 5 min by a sintering press DSP 25 ATS manufactured by Dr Fritsch Sondermaschinen GmbH. The graphite mould had a diameter of 1 cm and the applied pressure was 2·4 MPa. The mould chamber was evacuated to a pressure of $\sim 7{\cdot}0 \times 10^{-3}$ Torr. Electrical measurement on the sample exhibited a metallic conduction confirming the formation of a percolative chain of nanometre-sized copper particles.[8] Reduced gel powders prepared as above were heated in air at temperatures varying from 700 to 850°C for 30 min. This treatment was given to bring about oxidation of the copper particles.

For electrical property measurements samples were prepared after mixing metal- and oxidized metal-containing gel powders respectively prepared as described above in the weight ratio 48 : 52. This was done to lower the resistivity level of the resultant composite so that the temperature variation of resistivity could be studied conveniently. The mixture of these two powders in the above mentioned ratio was hot pressed at 650°C for 5 min by the procedure described earlier using a graphite mould of 1 cm diameter. The sample faces were ground with silver paste (supplied by Acheson Colloiden BV, Holland) and the DC electrical resistances were measured by 617 Keithley Electrometer over the temperature range 30 to 300°C under a vacuum of $\sim 10^{-2}$ Torr. A reference sample was also prepared by subjecting the gel powder (without being reduced) to a heat treatment at 650°C for 30 min for comparison of electrical resistivity with those of other specimens.

The microstructures of different specimens were studied by a JEM 200 CX transmission electron microscope. The details of specimen preparation have been described earlier.[9] The nanocrystalline phases within the samples were identified by analysing the diffraction rings obtained from selected area electron diffraction pattern.

3. Results and discussion

Figure 1a shows the transmission electron micrograph for the specimen reduced at 650°C for 30 min followed by oxidation treatment at 700°C for 30 min. Figure 1b is the electron diffraction pattern obtained from figure 1a. The interplanar spacing d_{hkl} values calculated from the diameters of the diffraction rings in the figure are listed in table 1 which also gives the standard ASTM data for Cu_2O, CuO and Cu respectively. It is evident from this

table that Cu_2O, CuO and Cu are present in these nanoparticles. Figure 2 shows the histogram of particle sizes obtained from figure 1a. The points in this figure represent the experimental data which have been fitted to a log normal distribution function. The theoretical curve is shown as the solid line in this figure. All the specimens studied here show similar characteristics. The extracted values of the median diameter $\bar{x}$ and the geometric standard deviation s for the different specimens are summarised in table 2. It is seen from these results that the median diameters as determined from the electron micrographs have lower values as the oxidation treatment is increased. This is reasonable to expect because copper oxide with a density lower than metallic copper will not be shown in the micrograph because of the contrast of electron density between the two phases. The micrographs therefore essentially record the diameters of metallic copper

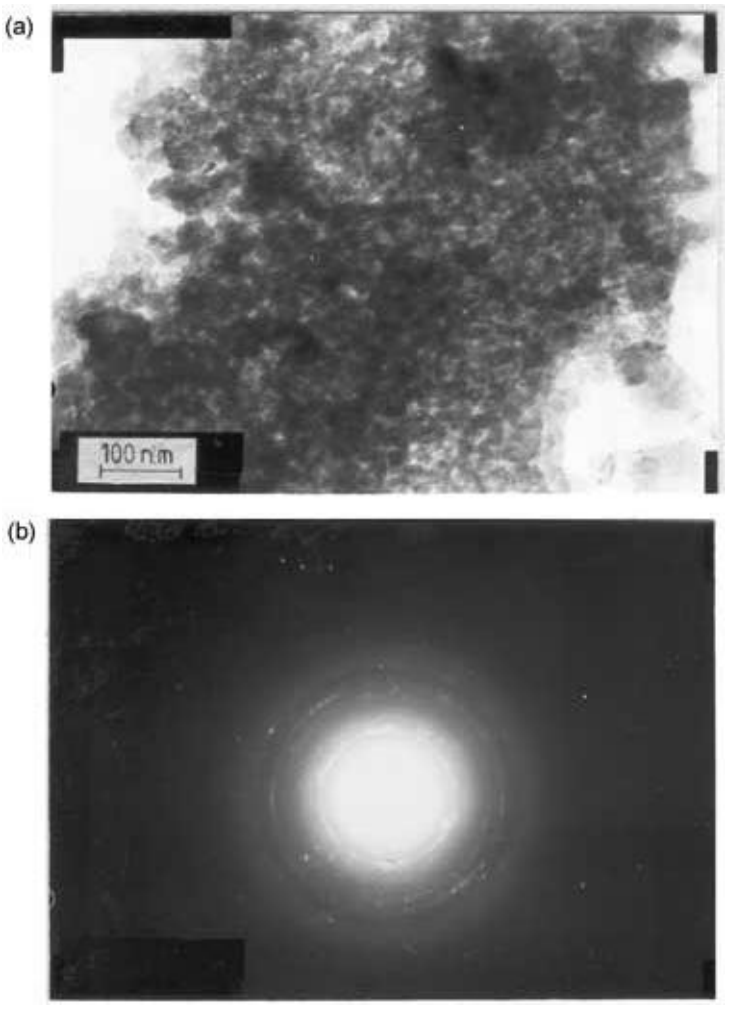

Figure 1. (**a**) Transmission electron micrograph for specimen prepared by reducing the precursor gel at 650°C for 30 min followed by oxidation at 700°C for 30 min. (**b**) Electron diffraction pattern for figure 1a.

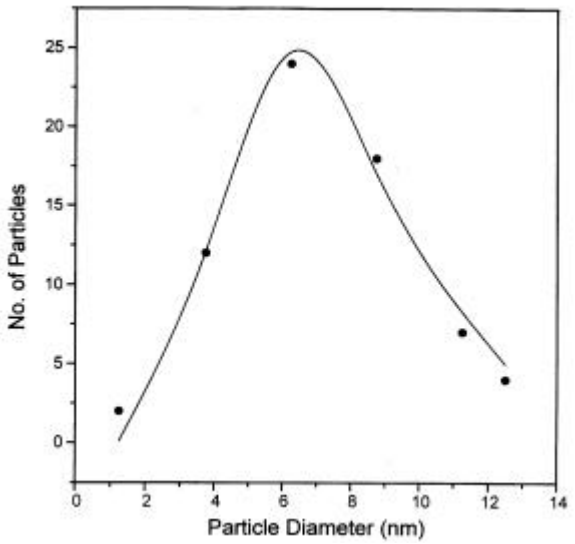

Figure 2. Histogram of particle sizes obtained from figure 1a.

Table 1. Comparison of d_{hkl} values obtained with ASTM data for specimens reduced at 650°C/30 min and then oxidised at 700°C/30 min.

	ASTM (nm)		
Observed (nm)	Cu_2O	CuO	Cu
0·246	0·2465	0·252	
0·211	0·2135	0·232	0·2088
0·164	0·1743		
0·148	0·1510		
0·127	0·1287		0·1278

Table 2. Summary of median diameter $\bar{x}$ and geometric standard deviation s for different specimens.

Specimen no.	Treatment schedule	Median diameter $\bar{x}$ (nm)	Geometric standard deviation s
1	Reduced at 650°C/30 min + oxidised at 700°C/30 min	7·3	1·5
2	Reduced at 650°C/30 min + oxidised at 800°C/30 min	6·9	1·5
3	Reduced at 650°C/30 min + oxidised at 850°C/30 min	6·1	1·7

cores. The electrical resistivity data discussed below indicate that the nanostructure consists of metallic copper with a copper oxide shell. The latter forms a percolative network.

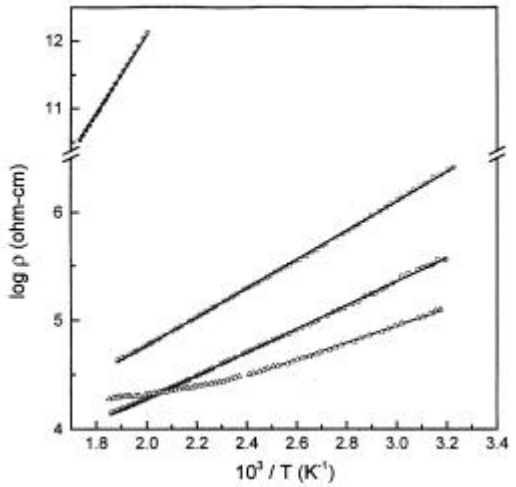

Figure 3. Log resistivity as a function of inverse temperature for different specimens. × Reference sample; □ specimen 1; □ specimen 2; specimen 3.

Figure 3 shows the variation of log resistivity as a function of temperature for the three specimens with different oxidation treatments. We also show the resistivity variation for the reference sample in this figure. It is evident that there is a drastic decrease in resistivity for specimens with a core-shell structure. The semiconducting behaviour exhibited by the latter rules out the possibility of any percolative metallic chain contributing to the transport behaviour. To explain the semiconductor-type transport we consider first the electron tunnelling mechanism between metallic islands separated by an insulating layer.[10] According to this model the activation energy for tunnelling is given by[11]

$$\phi = \frac{1 \cdot 44}{\varepsilon}[\{1/(x/2)\} - \{1/((x+s)/2)\}] \text{ eV}, \tag{1}$$

where x and s are the diameter of the metallic grain and the separation between grains respectively expressed in nanometres and ε is the dielectric constant of the intervening medium. Taking $\bar{x} \sim 5{\cdot}3$ nm, $s \sim 5.3$ nm and $\varepsilon \sim 10$, we obtain $\phi \sim 0{\cdot}04$ eV. For specimen no. 1 we find gradual lowering of activation energy as the temperature is increased. An activation energy $\sim 0{\cdot}07$ eV is estimated near the highest temperature measured. There is a change of activation energy at a lower temperature range which is $\sim 0{\cdot}18$ eV. This is discussed below as arising due to a small polaron hopping in the amorphous phase present at the interfaces of the nanosized copper oxide shell. Such a change of slope in the resistivity temperature plot has not been observed in the case of specimens 2 and 3. The nanosized metal particles introduced during the preparation of the composite are connected in series with the core-shell structure and hence will control the resistance change of the specimen in the temperature range where they contribute a higher resistance than the interfacial phase. In the cases of specimens 2 and 3 the oxidation treatments being higher than that for specimen 1 the oxide layer thickness also would be

large and therefore the activation energy for electron tunnelling would also be higher than that in specimen 1. As a result electron tunnelling in these samples in the temperature range concerned would contribute a smaller resistance than that in specimen 1. This is believed to be the reason why we do not observe any change of slope in the higher temperature range being discussed.

It has earlier been reported that in the gel derived silicate glass system containing copper small polaron hopping between nearest neighbours Cu^{+} and Cu^{2+} ions respectively contribute to electrical conduction.[12] We also note that the activation energies for the different specimens (except for specimen 1 in the higher temperature range) as obtained from the slopes of the log ρ vs $(1/T)$ curves in figure 3 are much smaller than that reported (~0·65 eV) from measurements on single crystals of Cu_2O.[13] Also it has been observed that the electrical resistivity of all the samples shows no change as a function of partial pressure of oxygen. This means that the semiconducting behaviour does not arise due to non-stoichiometry in Cu_2O.[14]

In view of the above discussion we analyse our electrical resistivity data on the basis of phonon-assisted small polaron hopping between Cu^{+} and Cu^{2+} sites. According to Mott's model[15] the conductivity ρ is given by

$$\rho = \frac{kTR}{\nu_0 e^2 C(1-C)} \exp(2\alpha R) \exp(+W/kT), \tag{2}$$

where ν_0 is the optical phonon frequency, c is the ratio of transition metal™ ion concentration in the lower valence state to the total TM concentration, α^{-1} is the localization length describing the localized state at each TM ion site, R is the average intersite separation and W is the activation energy for the hopping conduction. The experimental data for all the specimens were least square fitted to (2) and the extracted parameters are given in table 3. The points in figure 3 are the experimental data and the solid lines represent the theoretically fitted curves. It is seen from this table that the activation energy for hopping in the case of specimens 1, 2 and 3 are much smaller than that for the reference sample. Evidently the electrical transport in these samples arises due to the presence of an amorphous phase which is different from the precursor glass phase resulting from the gel formulation. We ascribe this phenomenon to an interfacial amorphous phase in between the nanosized Cu_2O-shells of the neighbouring grains. It should be noted that the Cu_2O shells form a percolative network in conjunction with the grains containing copper nanoparticles.

According to Austin–Mott model[15] the activation energy W can be approximately written as,

$$W = e^2/4\varepsilon_p\gamma_p, \tag{3}$$

where ε_p is the effective dielectric constant and r_p the polaron radius. The latter is given by,

$$r_p = (R/2)(\pi/6)^{1/3}. \tag{4}$$

We have estimated r_p values from (4) and substituting it in (3) and taking the experimentally obtained values of W, calculated the values of ε_p for the different specimens. It

can be seen that the ε_p values in the case of specimens containing copper core–copper shell nanostructure are much higher than that in the reference sample. This enhancement is ascribed to the presence of copper atoms in the confined geometry of the interfaces between the copper oxide nanoshells and also to the generation of high pressure at the interface as discussed in the following paragraph.

During the formation of copper oxide shell a high stress will be generated at the interface because of the fact that the densities of Cu_2O and copper are drastically different from each other viz., 6 g/cc and 8·92 g/cc respectively.[16] As a result when the Cu_2O layer is formed there should an effective expansion of the original particle which is prevented from taking place because of the presence of the neighbouring particles. Using the bulk modulus of copper we have calculated the effective stress which is generated on the composite particle as a result of this mechanism. By this analysis we calculate an effective pressure at the interface of these particles as of the order of ~ 40 GPa.

Dielectric properties of oxide glasses were measured at very high pressures previously.[17] Using a non-blocking electrode assembly dielectric relaxation spectra of both densified (at pressure ~ 2·0 GPa and temperature 500°C) and undensified glasses were delineated.[18,19] In figure 4 we show typical Cole–Cole plots for a specimen of composition 21·4 Na_2O, 7·2 Al_2O_3, 71·4 SiO_2 (mole%) in the two states. These glasses were prepared by a melt – quench technique. It can be seen that the dielectric constants at high frequencies as extracted from these plots are 12 and 8 for the densified and the virgin glass samples respectively. In the present specimen system we observe similar trends of data but in the nanoscale regime of specimen dimensions.

It is to be noted that the value of ε_p as estimated decreases as the oxidation treatment is increased. This apparent anomaly arises because of the presence of copper nanoparticles in the unoxidized gel while the mixture of the two powders is being compacted in the hot press at a temperature of 650°C. It is known that metallic copper reacts with cupric oxide to produce cuprous oxide.[20] It has been shown earlier that the copper oxide shell contains

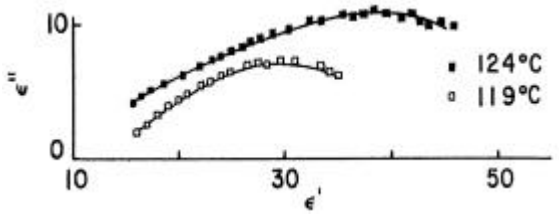

Figure 4. Cole–Cole plots for densified (by 1·13%) and undensified glass of composition 21·4 Na_2O, 7·2 Al_2O_3, 71·4 SiO_2 (mole%) obtained at a temperature of 120°C.[19] □ Densified; ■ undensified.

Table 3. Parameters obtained by fitting electrical conductivity data to Mott's model.

Specimen no.	W (eV)	a (A)	R (Å)	C	n_o (s^{-1})	ε_p (calc. from (3))
Reference	1·18	0·86	3·2	0·840	$9·2 \times 10^{12}$	4·7
1	0·19	0·60	3·7	0·998	$1·5 \times 10^{12}$	13·2
2	0·25	0·60	3·7	0·996	$2·5 \times 10^{12}$	9·8
3	0·30	0·57	3·5	0·997	$2·2 \times 10^{12}$	8·5

both Cu_2O and CuO. Since the gel particles containing core-shell structure are surrounded partly by particles containing copper nanoparticles the latter will react with CuO at the neighbouring grains. This will mean formation of Cu_2O shell on the copper nanoparticles. Reduction of the amount of CuO on the shell of the initially oxidised gel particle will therefore reduce the pressure at the interface. Such a reduction of pressure will lower the compaction of the interfacial amorphous phase thereby leading to a lower value of ϵ_p. Also the oxide layer formation on the initially unoxidized copper particles will increase the resistivity level of the nanocomposite. This is borne out by results shown in figure 3.

In summary, we have prepared nanostructured copper metal core–copper oxide shell within a silica gel by reduction followed by controlled oxidation of a suitable gel composition. The hot pressed gel powders mixed with nanosized copper particles dispersed in a silica gel show a marked enhancement in electrical conductivity as compared to that of the precursor gel. This is ascribed to the presence of an amorphous phase at the interfaces of the copper oxide shell. The activation energy of small polaron hopping in this phase is much lower than that in the original gel. The effective dielectric constant of the interfacial phase is estimated to be much higher than that of the original glass. This is ascribed to the generation of high pressure at the interface due to the processing steps involved.

Acknowledgment

The work was supported by Council of Scientific and Industrial Research, New Delhi.

References

1. Imry Y 1992 In *Nanostructures and mesoscopic systems* (ed.) W P Kirk and M A Reed (New York, London; Academic Press) p. 11
2. Boese D and Schoeller H 2001 *Europhys. Lett.* **54** 668
3. Tang Z K, Zhang L, Wang N, Zhang X X, Wen G H, Li G D, Wang J N, Chan C T and Sheng Ping 2001 *Science* **292** 2462
4. Jacobs K, Zaziski D, Scher E C, Herhold A B and Alivisatas A P 2001 *Science* **293** 1803
5. Konrad H, Karmonik C, Weissmuller J, Gleiter H, Birringer R and Hempelmann R 1997 *Physica* **B234**–**236** 173
6. Keblinski P, Phillpot S R, Wolf D and Gleiter H 1996 *Phys. Rev. Lett.* **77** 2965
7. Keblinski P, Wolf D, Phillpot S R and Gleiter H 1997 *Philos. Mag. Lett.* **76** 143
8. Roy S, Chatterjee A and Chakravorty D 1993 *J. Mater. Res.* **8** 689
9. Maity A K, Nath D and Chakravorty D 1996 *J. Phys. Condens. Matter* **8** 5717
10. Roy B, Roy S and Chakravorty D 1994 *J. Mater. Res.* **9** 2677
11. Tick P A and Fehlner F P 1962 *J. Appl. Phys.* **43** 362
12. Ghosh A and Chakravorty D 1993 *Phys. Rev.* **B48** 5167
13. Toth R S, Kilkson R and Trivich D 1961 *Phys. Rev.* **122** 482
14. Kingery W D 1967 *Introduction to ceramics* (New York: Wiley) p. 675
15. Austin I G and Mott N F 1969 *Adv. Phys.* **18** 41
16. Hodgman C D, Weast R C, Shankland R S and Selby S M (eds) 1962 *Handbook of chemistry and physics* (Cleveland, Ohio: Chem. Rubber Publ Co.) p. 568
17. Chakravorty D and Cross L E 1964 *J. Am. Ceram. Soc.* **47** 370
18. Chakravorty D and Cross L E 1965 *Rev. Sci. Instrum.* **36** 1151
19. Chakravorty D 1965 *Dielectric properties as a tool for the study of the densification of glass*, Ph D thesis, Pennsylvania State University, USA
20. Mellor J W 1952 *A comprehensive treatise on inorganic and theoretical chemistry* (London: Longmans & Green) vol. 3